Simultaneous laser beam combining and mode conversion using multiplexed volume phase elements

Marc SeGall*, Ivan Divliansky, Clémence Jollivet, Axel Schülzgen, and Leonid Glebov
The College of Optics & Photonics, University of Central Florida
*msegall@creol.ucf.edu

Abstract: To scale to power levels of up to tens of kW with a few fiber lasers, the best candidates are large core fibers guiding a few large-area higher order modes with the outputs of these fibers combined into a single beam. However, in many applications it is desirable to convert these higher order modes into a Gaussian profile. Here, we propose a method to accomplish this task via single volume phase element. This element accepts multiple higher order mode beams and simultaneously converts and combines them to a single Gaussian profile in the far field.

Keywords: Beam combining, mode conversion, phase mask, volume hologram

Introduction

Compact high-power lasers with good beam quality and narrow line-widths are desired for a great number of applications. Currently, 1 μm ytterbium-doped large area mode (LMA) fiber laser sources with several kilowatts of CW power in both single and multi-mode regimes are commercially available. However, further scaling to higher power levels is fundamentally limited due to the onset of thermal and nonlinear effects in the fiber. Spectral beam combining (SBC) and coherent beam combining (CBC) are the two major complementary methods of beam combining in the effort to reach multi-kilowatt diffraction limited beams [1-3]. Simultaneously with the progress of the beam combining techniques, a lot of effort has been put into designing and developing LMA fibers that support only one or few higher-order modes with the purpose of increasing the nonlinear effects threshold by increasing the effective fiber mode area. Of course, for long range propagation one will desire a pure fundamental (Gaussian) mode beam with M^2 parameter close to 1. To achieve power levels on the order of tens of kW with only a few fiber lasers, the best approach would be to use several large area high order mode fiber lasers whose outputs are later combined to a single beam and converted to the fundamental mode. Here, we propose a method to accomplish this task via single volume phase element. This element accepts multiple higher order mode beams and simultaneously converts and combines them to a single Gaussian beam.

Theory of Encoded Phase Masks

To encode the phase profile into a TBG, consider the recording setup in Fig. 1. Here a phase mask has been placed into one arm of a two-beam interference system, where the two beams interfere at an angle θ relative to the sample normal. The two-beam interference equation describing the fringe pattern in the sample will then be

$$I = I_1 + I_2 + 2\sqrt{I_1 I_2}\cos\left(\left(\vec{k}_1 - \vec{k}_2\right)\cdot\vec{r} + \varphi\left(x_0, y\right)\right), \quad (1)$$

where I is the intensity, $\vec{k}_i$ is the wavevector for each beam, and φ is the phase variation introduced by the phase mask after the object beam has propagated to the recording sample. If the thickness of the sample, the axial distance between the phase mask and the sample, and θ are small then $\varphi(x_0, y) \approx \varphi(x, y)$. The recorded TBG will therefore have a refractive index profile of $n(x, y, z) = n_0 + n_1\cos\left(\vec{K}\cdot\vec{r} + \varphi(x, y)\right)$, where n_0 is the background refractive index, n_1 is the refractive index modulation, and $\vec{K} = \vec{k}_1 - \vec{k}_2$ is the grating vector.

For a probe beam incident on the recorded hologram at or near the Bragg condition, the total electric field will satisfy the scalar Helmholtz wave equation,

$$\nabla^2 E - k_p^2 n^2 E = 0. \quad (2)$$

Laser Resonators, Microresonators, and Beam Control XVI, edited by Alexis V. Kudryashov, Alan H. Paxton, Vladimir S. Ilchenko, Lutz Aschke, Kunihiko Washio, Proc. of SPIE
Vol. 8960, 89601F · © 2014 SPIE · CCC code: 0277-786X/14/$18 · doi: 10.1117/12.2039753

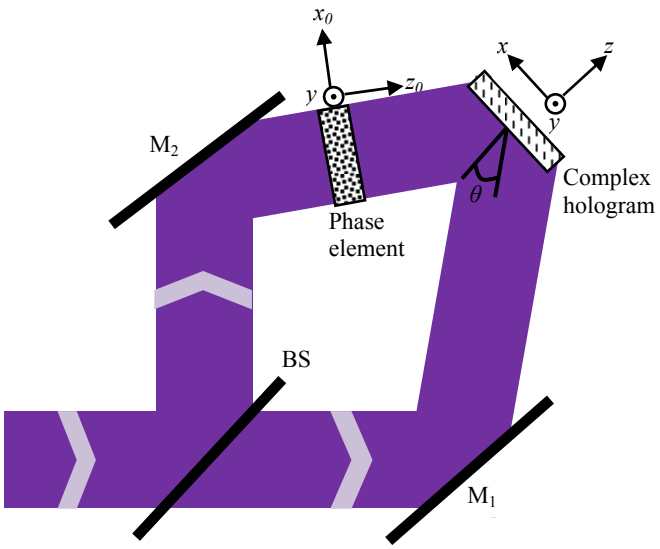

Fig. 1: Holographic recording of a phase mask.

Here k_p is the wavenumber of the probe beam. The Helmholtz equation has a general solution of the form [4]

$$E(x,y,z) = A(x,y,z)\exp\left(-i\vec{k}_p \cdot \vec{r}\right) + B(x,y,z)\exp\left(-i\vec{k}_d \cdot \vec{r}\right), \tag{3}$$

where A is the complex amplitude of the transmitted wave, B is the complex amplitude of the diffracted wave, and $\vec{k}_d = \vec{k}_p - \vec{K}$ is the wavevector of the diffracted beam. Inserting Eq. 3 into Eq. 2 will create a set of coupled wave equations between the amplitudes A and B. Kogelnik has solved these equations when A and B depend solely on the axial distance z [4], but because the phase term is not a constant when a phase mask is placed in the recording system it cannot be assumed that this one-dimensional dependence will still hold. For simplicity we will assume that the probe beam exactly satisfies the Bragg condition, as this case is the case of most interest to us. The coupled wave equations therefore become

$$\begin{aligned} \frac{1}{k_p}\left(k_{p,x}\frac{\partial A}{\partial x} + k_{p,y}\frac{\partial A}{\partial y} + k_{p,z}\frac{\partial A}{\partial z}\right) &= -i\kappa e^{-i\varphi(x,y)}B \\ \frac{1}{k_p}\left(k_{d,x}\frac{\partial B}{\partial x} + k_{d,y}\frac{\partial B}{\partial y} + k_{d,z}\frac{\partial B}{\partial z}\right) &= -i\kappa e^{i\varphi(x,y)}A \end{aligned}. \tag{4}$$

Here $\kappa=\pi n_1/\lambda_0$ is the coupling coefficient of the grating. Note that we have assumed that the second derivatives are negligibly small in the same manner as Kogelnik.

These coupled-wave equations cannot be solved analytically in the general case. To solve them numerically we will first convert Eq. 4 into Fourier space along the transverse dimensions, giving

$$\begin{aligned} \frac{2\pi i}{k_p}\left(f_x k_{p,x} + f_y k_{p,y}\right)\widetilde{A} + \frac{k_{p,z}}{k_p}\frac{\partial \widetilde{A}}{\partial z} &= F\left\{-i\kappa e^{-i\varphi(x,y)}B\right\} \\ \frac{2\pi i}{k_p}\left(f_x k_{d,x} + f_y k_{d,y}\right)\widetilde{B} + \frac{k_{d,z}}{k_p}\frac{\partial \widetilde{B}}{\partial z} &= F\left\{-i\kappa e^{i\varphi(x,y)}A\right\} \end{aligned}, \tag{5}$$

where $\tilde{A}$ is the Fourier transform of A and $\widetilde{B}$ is the Fourier transform of B. To solve these equations we will split the propagation and energy conservation into two discrete steps. To calculate the propagation of the beam assume that the right side of Eq. 5 equals zero. In this cased the amplitudes will have a solution of the form

$$\tilde{A}(f_x, f_y, z+\Delta z) = \tilde{A}(f_x, f_y, z)\exp\left(-i\frac{2\pi}{k_{p,z}}\left(f_x k_{p,x} + f_y k_{p,y}\right)\Delta z\right)$$
$$\tilde{B}(f_x, f_y, z+\Delta z) = \tilde{B}(f_x, f_y, z)\exp\left(-i\frac{2\pi}{k_{d,z}}\left(f_x k_{d,x} + f_y k_{d,y}\right)\Delta z\right) \quad (6)$$

Note that this only exact in the case where the right side of Eq. 5 equals zero but for small (~100 nm) propagation steps this is a reasonable approximation. The amplitude in real space is therefore the inverse Fourier transform plus the left side of equation 5:

$$A(x, y, z+\Delta z) = F^{-1}\left\{\tilde{A}(f_x, f_y, z+\Delta z)\right\} - i\kappa e^{-i\varphi(x,y)} B(x, y, z)\Delta z$$
$$B(x, y, z+\Delta z) = F^{-1}\left\{\tilde{B}(f_x, f_y, z+\Delta z)\right\} - i\kappa e^{i\varphi(x,y)} A(x, y, z)\Delta z \quad (7)$$

Calculations indicate that for a propagation step size of 100 nm energy is conserved to within 0.01%, which is sufficient for the phase profiles discussed here.

To determine the diffracted beam profile and diffraction efficiency in the case where a binary phase profile is encoded we simulated a grating with an 8 μm period, a refractive index modulation of 250 ppm, and a thickness of 2 mm. For a homogenous transmitting Bragg grating and a probe beam wavelength of 1064 nm, the diffraction efficiency is 99.13%. If a binary step is introduced, where the binary step is at a recording wavelength of 325 nm, then the diffraction efficiency will decrease by up to a few percent depending on the probe beam diameter and the orientation of the phase discontinuity relative to the probe beam propagation vector. This decrease in diffraction efficiency is caused by the step discontinuity, where it is not possible to satisfy the Bragg condition at 1064 nm. However, regardless of the diffraction efficiency and orientation of the phase discontinuity, in all cases the diffracted beam had a binary phase profile at 1064 nm. Therefore, as the decrease in diffraction efficiency is largely negligible for beam diameters larger than 1 mm, we conclude that ideal binary phase masks encoded into TBGs will allow for reconstruction of the phase profile at any wavelength capable of satisfying the Bragg condition with effectively the same diffraction efficiency as homogenous gratings.

Experimental Holographic Phase Masks

To experimentally verify these simulations, holograms of a four-sector mode converting mask (chosen to give a binary phase shift along the horizontal and vertical axes in a single element) were recorded using a Mach-Zehnder-type recording system in 1.97 mm-thick photo-thermo-refractive (PTR) glass. PTR glass is a photosensitive glass which has been used in a variety of applications, including producing volume phase masks [5] and beam combining [1-3]. A four-sector mode converting mask (partially converting a Gaussian beam into the TEM_{11} mode) designed for the recording wavelength of 325 nm was placed in one arm of the setup shown in Fig. 1 and the half angles of interference chosen to give an 8 μm grating period.

After the recording the volume phase mask the diffracted beam was then examined in the far field (achieved by focusing the beam with a 500 mm lens) at multiple wavelengths in the visible and the infrared regions using a 3 mm

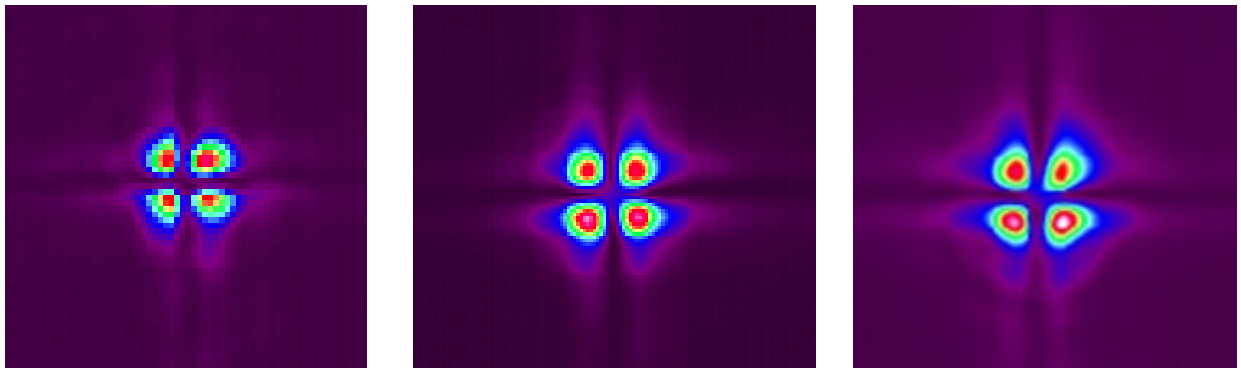

(a) (b) (c)

Fig. 2: Far field profile of the diffracted beam after propagating through a holographic four-sector mode converting mask at (a) 632.8 nm, (b) 975 nm, and (c) 1064 nm. The sizes shown here are not to scale.

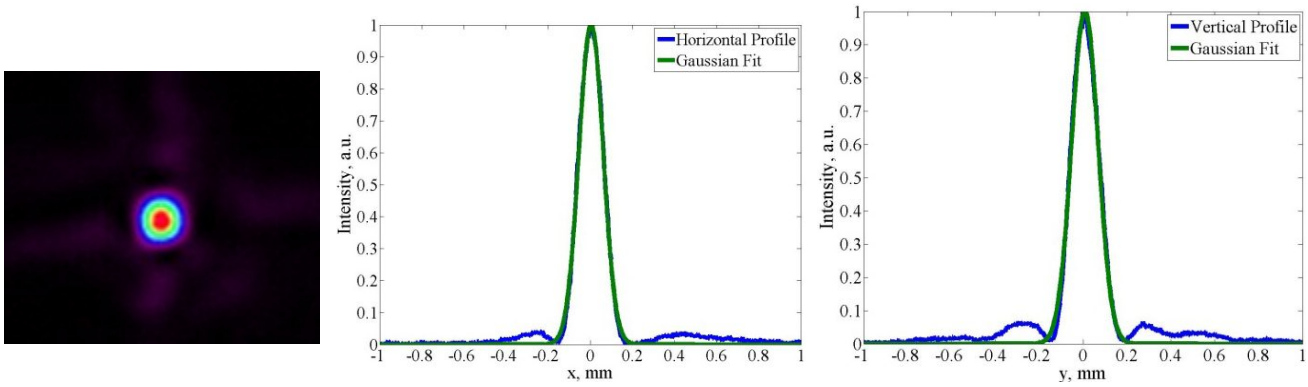

(a) (b) (c)

Fig. 3: (a) Far field profile of a beam converted from a higher order mode to a Gaussian profile. (b) Horizontal and (c) vertical cross sections of the beam indicate that the central spot is nearly diffraction limited.

probe beam to determine the wavelength dependence of mode conversion. As shown in Fig. 2, in all cases the diffracted profile exhibited the same four-lobed pattern. The profiles in Fig. 2 are very similar to the far field profile of the four-sector volume phase mask in [5], indicating that there is a mode converting element encoded into the volume grating.

The mode converting ability of the phase masks is of course not limited to converting a Gaussian beam to a higher order mode; it is also possible to convert from a higher order mode to a Gaussian profile. To demonstrate this, two 4-sector mode converting holographic phase masks were aligned so that a 3 mm Gaussian beam at 1064 nm was incident on the first mask and the diffracted (converted) beam from this mask was incident on the second converter. This doubly converted beam was then focused by a 500 mm lens to achieve the far field profile. As shown in Fig. 3a, the far field profile is a Gaussian spot with some low-energy side lobes. Cross sections of the beam, shown in Fig. 3b and 3c, were fitted with Gaussian functions to determine the size of the main spot relative to a diffraction-limited spot. The fits indicate that the spot size along the horizontal axis is 228 μm, nearly identical to the diffraction-limited spot size of 226 μm, while the spot size along the vertical axis is 240 μm, which is close to diffraction-limited. The wings are caused by the finite transition regions at the boundary between the different grating phases and can be reduced by reducing the size of the transition regions in the original phase mask used for recording as well as placing the phase mask closer to the sample during recording.

The diffraction efficiency of these volume phase masks can be compared to a homogenous grating by multiplexing a homogenous grating and volume phase mask in a single element. This was done by recording a volume phase mask in the setup shown in Fig. 1 and then removing the phase mask in the object beam and rotating the PTR

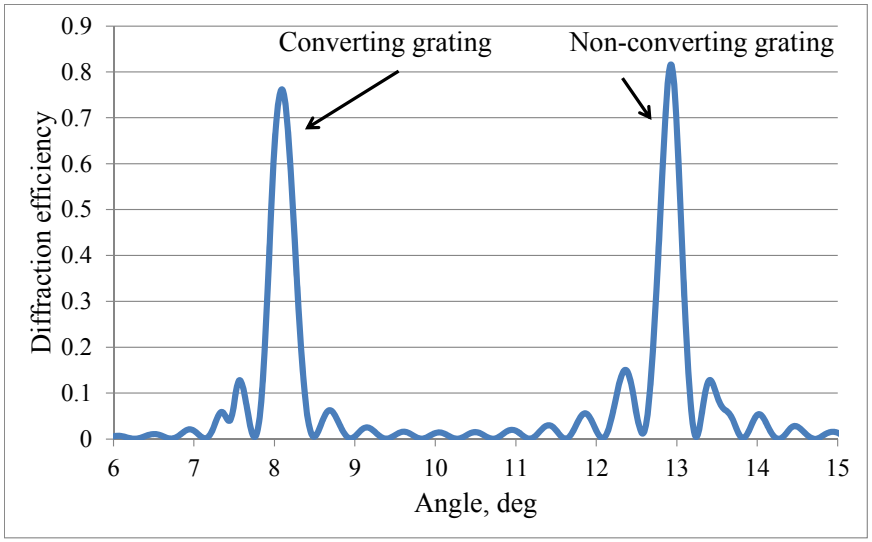

Fig. 4: Diffraction efficiency of a volume phase mask converting a Gaussian beam to the TEM_{11} mode compared to the diffraction efficiency of a homogenous grating.

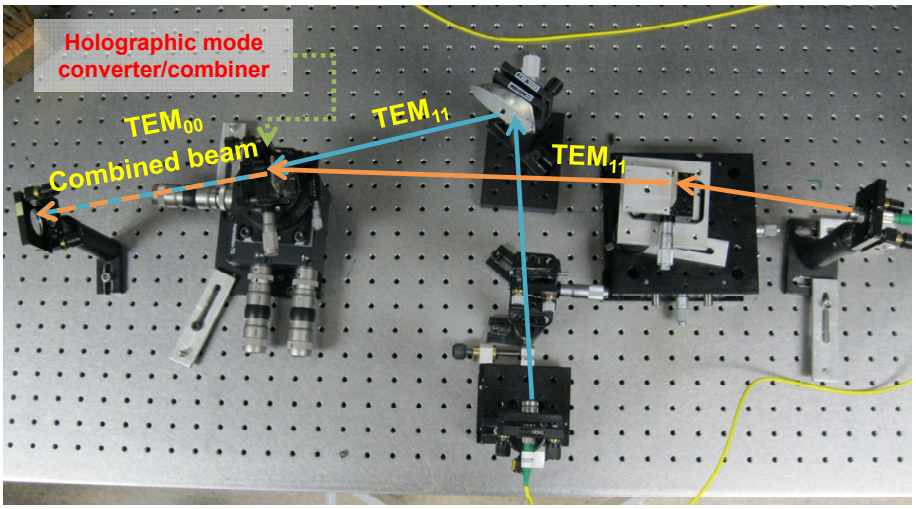

Fig. 5: Two multiplexed volume phase masks diffract incident beams into a common port while simultaneously converting the beams from the TEM_{11} mode to a Gaussian beam.

sample to record a homogenous grating. As shown in Fig. 4, the diffraction efficiencies of each element are approximately the same, showing good agreement with theoretical predictions.

Simultaneous Mode Conversion and Beam Combining

Having demonstrated that the holographic phase masks will reproduce the desired phase distribution in the diffracted beam with comparable diffraction efficiency as a homogenous grating, it is possible to perform simultaneous beam combining and mode conversion using multiplexed volume holographic phase masks. As shown in Fig. 5 we converted two Gaussian beams, one at 1064 nm and the other at 1061 nm, to higher order modes using volume holographic masks and then spectrally combined the resulting beams while simultaneously converting them back to the Gaussian mode with a multiplexed holographic phase mask element. Note that the combined beam will only have a Gaussian profile in the far field since the converting element is binary; for a Gaussian profile at arbitrary propagation distances after the combining element it is necessary to have a more complex phase distribution.

The far field intensity profile of the combined beam, shown in Fig. 6a, shows good beam combination and a fair conversion to the Gaussian mode, with some wings remaining in the combined beam. These wings are predominantly caused by the poor conversion of one of the beams by the combining element, shown in Fig. 6b. This poor conversion is a result of using volume holographic masks to convert the initial Gaussian beams to the TEM_{11} mode and can be improved by using a spatial light modulator or other phase element for the initial conversion.

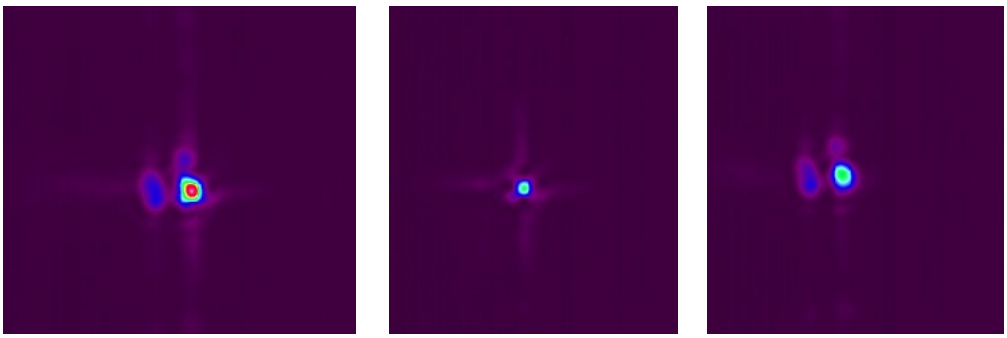

(a) (b)

Fig. 6: (a) Combined beam converted from the TEM_{11} mode to a Gaussian spot, and (b) the combined beam decomposed into its constituent beams.

Conclusions

We have successfully demonstrated that binary phase profiles may be encoded into volume Bragg gratings, and that for any probe beam capable of satisfying the Bragg condition of the hologram this phase profile will be present in the diffracted beam. A multiplexed set of these holographic phase masks can simultaneously combine incident probe beams in the same manner as homogenous multiplexed gratings while simultaneously converting the incident beams into a desired mode. This allows for high power diffraction limited spots by using large mode area fibers, capable of transmitting higher powers than single-mode fibers without nonlinear effects becoming predominant, and containing only one or a few higher order modes, to be used as the input elements, with the mode converting element restoring the Gaussian spot. This will significantly reduce the number of elements needed to create a high power fiber delivery laser system.

This work is supported by the Air Force Office of Scientific Research through grant No. W911NF-10-1-0441.

References

1. Divliansky, I., Ott, D., Anderson, B., Drachenberg, D., Rotar, V., Venus, G., and Glebov, L., "Multiplexed volume Bragg gratings for spectral beam combining of high power fiber lasers", Proceedings of SPIE **8237**, 823705 (2012).
2. Lu, C., Flores, A., Bochove, E., Roach, W., Smirnov, V., and Glebov, L., "Coherent beam combination of fiber laser arrays via multiplexed volume Bragg gratings," CLEO: Science and Innovations, OSA Technical Digest, CF2N.2 (2012).
3. Jain, A., Spiegelberg, C., Smirnov, V., Glebov, L., and Bochove, E., "Efficient coherent beam combining of fiber lasers using multiplexed volume Bragg gratings," CLEO: Science and Innovations, OSA Technical Digest, CF2N.8 (2012).
4. Kogelnik, H., "Coupled wave theory for thick volume holograms," Bell System Tech. J. **45**, 2909-2944 (1969).
5. SeGall, M., Rotar, V., Lumeau, J., Mokhov, S., Zeldovich, B., and Glebov, L., "Binary volume phase masks in photo-thermo-refractive glass," Opt. Lett. **37**, 1190-1192 (2012).